

Dosimetric evaluation of brain radiotherapy using custom-made Rhizophora head phantom – comparison between Monte Carlo GATE and treatment planning system MONACO

**S.H. Zuber^{1*}, M.F.R. Abdul Hadi², N.A.A. Hashikin², D.O. Samson³,
N.H. Ishak⁴, N.A. Raof⁴, M.Z. Abdul Aziz⁴, M.F.M. Yusof⁵, N.A. Rabaiee⁶**

¹Centre for Diagnostic, Therapeutic and Investigative Studies, Faculty of Health Sciences, Universiti Kebangsaan Malaysia, Kuala Lumpur, Malaysia

²School of Physics, Universiti Sains Malaysia, Penang, Malaysia

³Department of Physics, Faculty of Science, University of Abuja, Abuja, Malaysia

⁴Advanced Medical & Dental Institute, Universiti Sains Malaysia, Penang, Malaysia

⁵Faculty of Health and Life Sciences, Management & Science University, Selangor, Malaysia

⁶Department of Radiology, Kulliyah of Medicine, International Islamic University Malaysia, Gombak, Malaysia

► Original article

***Corresponding author:**

Siti Hajar Zuber, Ph.D.,

E-mail:

hajarzuber@ukm.edu.my

Received: September 2023

Final revised: April 2024

Accepted: May 2024

Int. J. Radiat. Res., January 2025;
23(1): 13-20

DOI: 10.61186/ijrr.23.1.13

Keywords: Dosimetry, brain radiotherapy, Monte Carlo simulation, treatment-planning system, GATE.

INTRODUCTION

Brain metastases are a common sign of systemic cancer, which is one of the most typical intracranial tumours in adults, outnumbering primary brain tumours. They are among the key contributors to neurologic disorders and affect 20% to 40% of all cancer patients^(1,2). Previous literature has identified brain metastases as the primary factor in patient morbidity and mortality⁽³⁾. It subsequently highlights the prominence of radiotherapy to improve the patients' quality of life.

Treatment accuracy is a crucial aspect for radiotherapy's efficiency in treating brain metastases, particularly in giving tumours the highest achievable dose while avoiding unneeded doses to normal tissues. Whole brain radiotherapy continues to be a cornerstone of patients' palliative care^(4, 5). Regression of the lesions' report after whole brain irradiation was discovered to correspond with survival and better neurocognitive performance⁽⁶⁾. Therefore, the primary goal of treatment is to control

ABSTRACT

Background: A custom-built head phantom has the potential as a dosimetric phantom in brain radiotherapy. **Materials and Methods:** Computed tomography (CT) was used to scan the phantom with CT data imported to treatment planning system (TPS) for dose computation. The dose prescription was pre-determined to deliver 300 cGy per fraction to the isocenter of the beam. 6 MV photon with parallel-opposed technique was used in this work. Absorbed dose computed in planning target volume (PTV) and organ at risks (OARs) were computed, and comparison was made with Monte Carlo (MC) Geant4 Application for Tomographic Emission (GATE). **Results:** The result demonstrates a close proximity of computed dose for TPS and GATE with a 1.6 % discrepancy for the PTV, with less than 1 % statistical uncertainty for GATE. The dose measured by TPS for most of the target of interest was in close proximity with the dose measured in MC. **Conclusion:** This study revealed the potential of MC GATE simulation in the dosimetric evaluation and verification of the treatment planning.

macroscopic lesions.

Recent technological developments enable various sectors to rely on algorithms, electronic, or digital data to promote high-quality industry operation and output. The algorithm marketability and use of electronic data are growing at an exceptionally fast rate, and this popularity boom has attracted numerous research and studies concerning the application of algorithms across a wide range of fields. As algorithm use in clinical dosimetry and quality control gained popularity in the healthcare sector, it was found to be precise, effective, and closely aligned with experimental measurements. As a result, using simulation in research involving radioactive sources has become essential and its efficiency stands as a determinant of the research development.

Previous literature reported that MC algorithm is the gold standard for calculating absorbed dosage⁽⁷⁾. GATE or 'Geometry and Tracking' aids in simulating particle movement through matter with MC techniques. In particular, the GEANT4 particle

simulation toolkit has been gaining popularity in the field of medical physics. It employs C++ code that allows for object-oriented programming and can thus model and simulate particles' interactions with matter. This will ease the addition of new processes, shapes, graphic drivers, and other features.

GATE was developed by the international OpenGATE collaboration as an open-source simulation framework that allows for easy simulation of imaging, radiation, and dosimetry in a single environment ^(8, 9). The cutting-edge software is capable of simulating the interaction between identical or dissimilar matters as part of the GEANT4 toolbox. It also offers high-level capabilities to facilitate simulation and design without the requirement for C++ programming, which can be complex and challenging to understand. The smooth and simple building of geometry in GATE leads to precise simulation in a realistic setup owing to a dedicated scripting mechanism ⁽¹⁰⁾. Additionally, the validation by GATE has proven its dependability in dosimetry and radiation treatment ⁽¹¹⁾.

An essential evaluation tool for every radiation therapy treatment is a radiation treatment plan with precise and reliable dose computation ⁽¹²⁾. The treatment planning system (TPS)'s choice of dosage calculation method will affect the treatment plan. This is because the estimated dose from multiple TPSs must be precise and consistent across different TPSs and better precision could be achieved with technological advancement. Furthermore, using phantom with allocation for dosimeters is crucial for the secure and effective execution of treatment ⁽¹³⁾.

In this work, the treatment plan for brain irradiation was evaluated using the MC GATE simulation. A novel, custom-built head phantom consisting of soy-lignin *Rhizophora* spp. was created and the absorbed doses to the target and organ at risks (OARs) were determined using TPS and GATE. The validation would reveal any discrepancies between experimental and simulated doses in the target volume as well as potential issues with the assumed properties of the head phantom in a simulation or experimental setup. The findings will serve as a useful guide for further verification of treatment planning for complex radiotherapy techniques.

MATERIALS AND METHODS

Preparation and fabrication of custom-made head phantom

Wood particles with soy flour and lignin adhesives were hot pressed at approximately 200 °C to fabricate a particleboard for the production of phantom material. Past studies investigated and analysed the selection and characterisation of the soy-lignin *Rhizophora* phantom ⁽¹⁴⁻¹⁸⁾. Following

RANDO® phantom, the particleboards were cut into the desired shape and each slab received a gloss treatment to achieve smoothness. A total of 20 head phantom slabs, each measuring around 1.0 cm in thickness, were produced accordingly.

Treatment planning for brain radiotherapy

The custom-built head phantom was scanned with a CT simulation scanner, Toshiba Aquilion (Toshiba Medical Systems, Japan), at the Oncology and Radiotherapy Unit, Universiti Sains Malaysia (USM) Medical Centre. The purpose was to gather CT raw data for the MONACO treatment planning process. Phantom CT images were used to characterise the target volume and normal structures, allowing the planning and delivery system to be as effective as possible. The intended treatment plan was then conducted, followed by a comparison of the measured and computed dosages.

TPS MONACO (Elekta, Sweden) was used to identify the target area and many organs at risk, including eyes, lens, optic nerves, brainstem, spinal cord, and parotid glands. To account for uncertainties, a 1.0 mm margin was introduced to the optic nerves and brain stem, which were called planning organ at risk volume (PRV). Meanwhile, a 5.0 mm margin was introduced for the spinal cord. Previous literature reported that a 5% dosage adjustment can result in a considerable change in cancer control and normal tissue complication risks ⁽¹⁹⁾. TPS recorded the dose volume histogram (DVH), which was then compared with the GATE simulation. The conformity index (CI), which depicts the link between isodose distributions and target volume, can be utilised to evaluate the quality and conformality of a treatment plan ⁽²⁰⁾. A high PTV coverage and minimal needless irradiation of nearby tissues are indicated by a conformance index of unity. It is recommended to quantify CI because it may be influenced by both planning variables and tumour characteristics ⁽²⁰⁾. Equation 1 defines the calculation for CI ⁽²⁰⁾.

$$CI = \frac{TV}{PTV} \quad (1)$$

Where; *TV* is the treated volume and *PTV* is the planning target volume. *TV* is the tissue volume that received at least the dose determined and stated to fulfil the goal of the therapy, such as the treated volume encompassing the 95% isodose ^(20, 21). Using information from the DVH and the RTOG 90-05 procedure, the treated volume (i.e., the volume of tissue enclosed by the 95% isodose) was computed ⁽²²⁾.

Simulation using GATE and comparison of dose between TPS and GATE

The linear accelerator with precise multileaf collimators was utilised to model and simulate the

radiation treatment. The phantom was modelled using the extracted CT raw data and the dose calculation was measured appropriately. Six MV of energy was taken into account for photons. The dosage computed by TPS MONACO was compared to the absorbed dose obtained from GATE. Figure 1, shows the exported data from CT displayed in 3D Slicer in preparation for GATE.

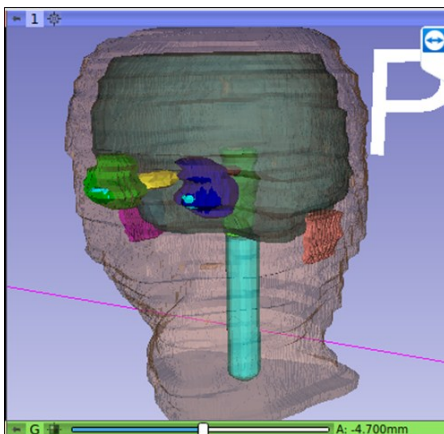


Figure 1. CT data with segmented organ of interest illustrated in 3D Slicer.

Following the planning in TPS MONACO, all beam configurations were recorded in 3D Slicer. The CT data was saved in the *mhd* format after being visualised in 3D Slicer to ensure compliance with the Monte Carlo GATE code. It was later imported as patient *mhd*, a voxel phantom placed in the centre of the world. Schneider 2000 table conversion was used to convert the Hounsfield unit conversion to a material database (23). The computer model utilised was an HP-Z8-G4-Workstation running Ubuntu 20.04 LTS with an Intel Xeon Gold 6242 (16 cores, 32 threads). In this work, GATE version 9.1 and Geant4 version 10.6 patch 3 were installed and the GATE's input file simulated the experimental setup by employing macro files containing a collection of commands.

The absorbed doses measured by TPS and GATE were collected and compared to determine the percentage discrepancy. Statistical uncertainties for the MC GATE simulation were calculated automatically by GATE. However, as a reference in the MC-generated model, the calculation of statistical uncertainty in dose was determined using equation 2 (24).

$$s_{\bar{d}_k} = \sqrt{\frac{1}{N-1} \left(\frac{\sum_{j=1}^N d_{k,i}^2}{N} - \left(\frac{\sum_{j=1}^N d_{k,i}}{N} \right)^2 \right)} \quad (2)$$

Where; $s_{\bar{d}_k}$ is an estimate of the standard error of the mean dose in voxel k , $d_{k,i}$ is the dose deposited in voxel k by independent history i , and N is the total number of primary independent histories. The GATE simulation output produced the dosage image, which was predetermined at 5.0 mm voxel size to match the TPS-specified voxel size. The resulting dosage image

was attached to the custom-built phantom.

RESULTS

Preparation and fabrication of custom-made head phantom

In this work, the custom-made head phantom was fabricated and the final outcome is illustrated in figure 2. The formulation of *Rhizophora* bonded with 12% soy flour and lignin with gloss finish coating was chosen for the fabrication of the phantom based on previous works (17,25). The head phantom was marked from A to T, resulting in a total of 20 slabs.

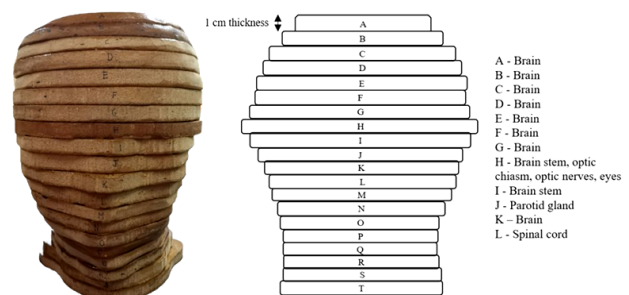


Figure 2. Custom-made soy-lignin bonded *Rhizophora* spp. head phantom fabricated in this work.

Treatment planning for brain radiotherapy

The treatment planning in this work was designed to provide 3000 cGy in 10 fractions, with 300 cGy per fraction to the custom-built head phantom, using the Elekta Synergy linear accelerator (Elekta, Sweden). The dose was targeted at the beam's isocenter. 6 MV photon was selected using a parallel-opposed approach with two beams arrangement with the CI value was recorded at 1.00.

Simulation using GATE and comparison of dose between TPS and GATE

For GATE simulation, the linear accelerator specification was necessary to design a precise treatment head for GATE, including particular shape, dimension, position, beginning energy, and material composition (26). Component module is a component of an individual treatment head that consists of several elements and certain geometrical shapes. The geometry of the linear accelerator's head was created to vendor specifications and the design was developed based on earlier literature. In this work, the mean electron beam energy of 6.4 MeV and 3.0 mm electron spot best fit the data with percentage depth dose (PDD), demonstrating a 100% pass for gamma comparison with the 3%/3mm criteria.

In GATE, phase space was employed to record the energy spectrum and the results were saved as ROOT files. Phase space was also utilised for the simulation and determination of PDD and beam profile for the *Rhizophora* material. Figures 3 to 5 show the linear accelerator's model geometry used in GATE simulation while Figures 6 and 7 illustrate the linear accelerator's model where the simulation took place.

The MC reports in this work adhered to Task Group 268⁽²⁷⁾ as shown in table 1. The beam geometry from one gantry angle was duplicated using the identical source-axis distance value. The data was normalised for planning target volume at 30 Gy prescribed dose. The *DoseActor* was coupled with the head phantom to generate a dosage image, which was then processed using 3D Slicer with the segmentation volume from TPS.

Figure 8 compares the dosages measured with TPS MONACO, TPS measured with GATE, and MC GATE simulation. All OARs and PTV are within dose constraints except parotid, with optic nerves (25.34 - 26.28) Gy with a constraint of 55 Gy, eyes (7.78 - 7.87) Gy with a constraint of 45 Gy, optic chiasm (29.12 Gy) with a constraint of 54 Gy, brainstem (29.18 Gy) with a constraint of 54 Gy, spinal cord (2.38 Gy) with a constraint of 45 Gy, and PTV (30.00 Gy) with a constraint of 65 Gy.

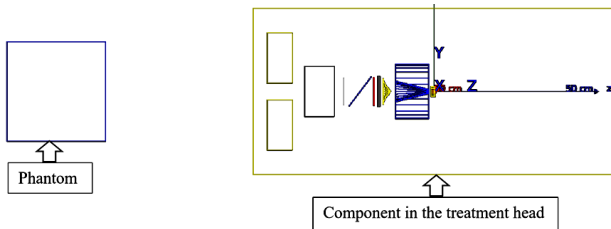


Figure 3. Linear accelerator modelling prepared in the MC GATE simulation.

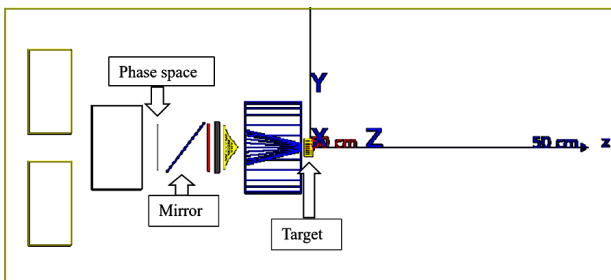


Figure 4. Treatment head simulated in MC GATE.

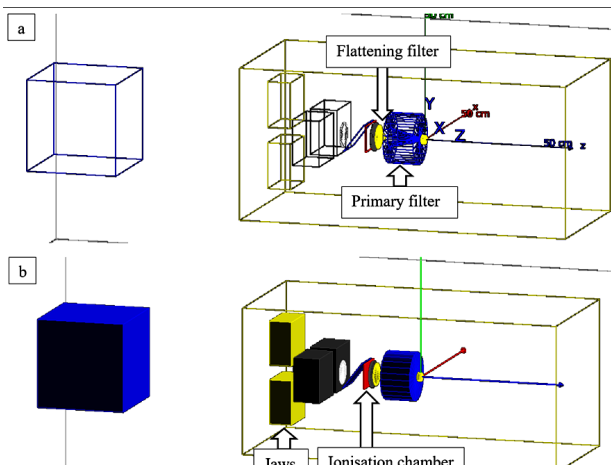


Figure 5. (a, b), 3D view of the treatment head modelling simulated in GATE.

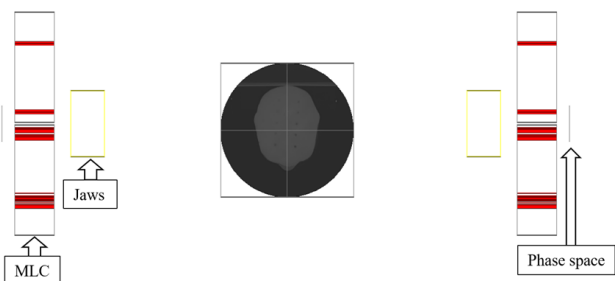


Figure 6. Bird eye view of the phantom in the linear accelerator setting with the right and left beams reflect the lateral opposing field.

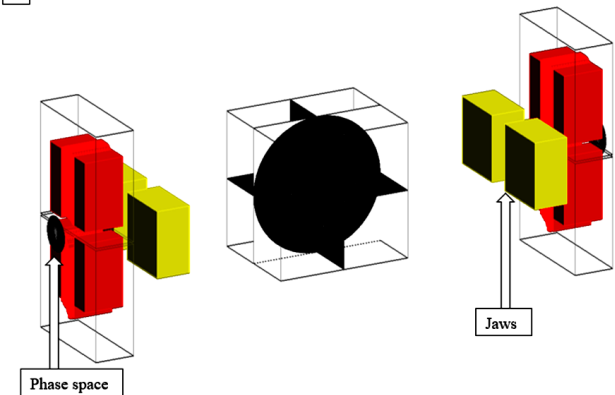
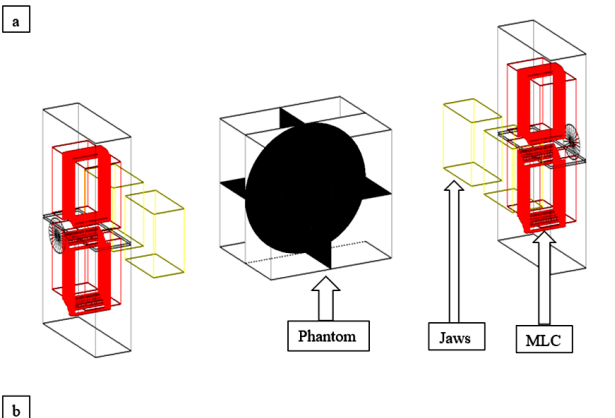


Figure 7. (a, b), Full overview of the linear accelerator with phantom in position for the GATE simulation, where the simulation began with the phase, as photons passed through the multileaf collimator and jaws and were directed towards the phantom in the centre.

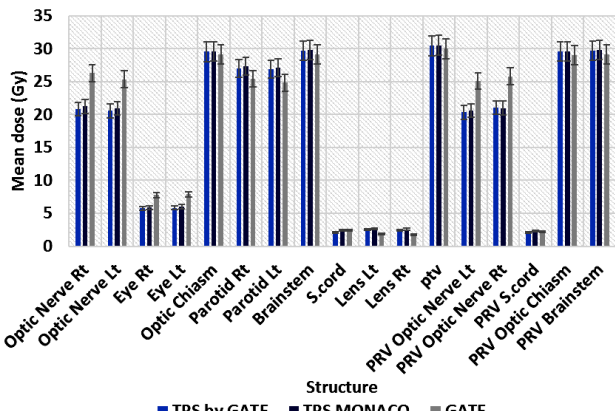


Figure 8. Comparison of dose measured using TPS MONACO, TPS measured by GATE and MC GATE simulation. Rt = right; Lt = left; ptv = planning target volume; PRV = planning organ at risk volume; Error bar = 5 % percentage error

Table 1. RECORDS items checklist for MC study.

Checklist item #	Item name	Description
2, 3	Code, version/release date	GATE v9.0 with geant4 v10.06.p03 and Root v6.24/0 platform Release Date: 03/02/2020
4, 17	Validation	Code was being validated against experimental measurements (Linear accelerator configuration based on Elekta Synergy Agility LINAC (Elekta Medical Systems, Crawley, UK)
5	Timing	CPU based simulation: 3.9 GHz and 32 threads CPU CPU/GPU model number: Intel Xeon Gold 6242 NVIDIA Quadro P2200
8	Source description	Source of phase-space: Energy spectrum from interaction gamma radiation Model parameter value: Nil
9	Cross-sections	Cross-section data: Nil
10	Transport parameters	EM Standard Option 4 (geant4) & secondary production cut-off 0.1 mm
11	VRT and/or AEIT	Nil
12	Scored quantities	DoseActor
13, 18	# histories/statistical uncertainty	Range of histories used was 2×10^9 / uncertainties of < 2 % for 150 million histories
14	Statistical methods	Statistical uncertainties measured based on equation (automatically generated in GATE)
15, 16	Postprocessing	Nil

LINAC = linear accelerator; UK = United Kingdom; CPU = central processing unit; GPU = graphics processing unit; EM = electromagnetic; VRT = variance reduction technique; AEIT = approximate efficiency improving technique

DISCUSSIONS

Based on the average CT numbers, relative electron density (RED), and CT density profile, the quality of the custom-built particleboard was analysed and the results revealed close compatibility with water. Particleboard has the potential as a phantom material, as evidenced by the mass attenuation coefficient's close proximity to water from the XCOM database. Results of the elemental composition analysis and effective atomic number calculation showed that *Rhizophora* particleboard with soy-lignin bonds has the potential to be used as phantom materials since its effective atomic number values were near to water's *Zeff* value⁽¹⁸⁾.

Previous research suggested that phantoms constructed of a material that closely resembles soft tissue should be employed to effectively analyse the patient contour and validate the radiotherapy techniques at both the commissioning and clinical stages. The calculated radiation dose for the phantom and the actual measured radiation dose can be compared by exposing the phantom to a series of beams. These phantoms should have radiologic characteristics that are identical to those of the tissues in question, anatomical realism, and the ability to use a variety of measuring devices to confirm dose and its distribution across various crucial locations throughout the target and normal tissue volumes⁽²⁸⁾.

Delineation of the target area and OARs is the first step in the planning method for radiotherapy. Additional margin was included to the target volume and OAR to account for the movement of patient and organ as well as differences in positioning. Additional space will lessen the likelihood of inaccurate beam positioning and beam direction at the target area.

The dose volume histogram (DVH) specifies the three-dimensional (3D) dose distribution inside the

treatment volume with maximum, mean, and minimum values to the target of interest^(29,30). Since DVH may also generate isodose curves around certain percentages of target volume and healthy tissues, it stands as a useful analytical tool for interpreting the dose distribution in target volume^(30,31). DVHs facilitated the treatment planning and ensured that the 95% PTV was completely covered by the 95% isodose while minimising the dose to healthy tissues⁽²⁰⁾.

The utilisation of parallel fields in whole brain irradiation allows for full coverage⁽³²⁾. The beam arrangement and weighting were adjusted so that 95% of the dosage covered 95% of the PTV volume, which was aligned with the recommended target dose uniformity of +7% and -5% by the International Commission on Radiation Units and Measurements (ICRU) Report 50⁽³³⁾.

The outcome of this study showed that the TPS's CI value was 1.00, which is in good agreement with the ideal value and may enable improved conformity of the dose region to PTV. This index may also indicate how closely the dose region adheres to the target volume, usually PTV. A CI number exceeding 1 shows that TV is larger than PTV, making it less conformal; a CI value less than one indicates that PTV is not totally covered by 90% isodose and hence cannot comply with ICRU 50⁽²⁰⁾. A good therapeutic index may be conferred by good conformance indices⁽²⁰⁾, with a better plan adhering to the target of interest can potentially provide a curative approach in radiotherapy. However, CI might not offer enough details regarding the entire treatment plan and the index might not account for the volume of surrounding healthy tissues⁽²⁹⁾.

The precision of radiation dose delivery has been reported and reviewed in earlier literature by ICRU. Past research suggests that radiation dose delivery errors of 5 % should be satisfied by dosage

uncertainties in photons that are less than 2% (34). The precision of dose delivery during radiotherapy treatment was intended to be better than $\pm 5\%$, and for this to be achieved, the accuracy of dose computation must not exceed $\pm 3\%$. However, previous literature postulated that existing algorithms frequently produce greater variances or deviations (35,36). For inhomogeneous tissues or irregular surfaces, it is commonly acknowledged that advanced algorithm has the capacity to handle the issues with great precision and can also produce a good solution. Meanwhile, the arrangement of the beam geometry closely followed the TPS plan with phase space employed to capture all photon data from the treatment head, which was then directed to the treatment area for the final output. One geometric component of a linear accelerator that is challenging to model is the multileaf collimator, which can only be properly simulated using MC techniques; however, this is not a simple operation. To reproduce similar opening during the simulation, the segment details of the x - and y -axis were individually extracted from TPS into Microsoft Excel, rechecked, rescaled to fit the requirement in GATE, and entered into the simulation.

The photon spectra and cross sections, including statistical uncertainties, are additional potential sources of uncertainty in MC simulation. Past literature suggests that for less than 2% uncertainties with 150 million histories, the simulation's statistical uncertainty was less than 1% (24). When evaluating TPS dosimetry in various complicated geometries, the MC technique is highly preferred (37) as it offers more comparison points than can be measured precisely. This will enable the application of more advanced methodologies into the analysis, resulting in a better, more thorough dosimetric evaluation of the dosage calculation algorithms (37). However, a disadvantage of this benefit is that it may allow for higher variances than those measured empirically due to the larger number of comparison points (37).

All MC calculations rely largely on input from human expertise in addition to the algorithm and technology. The onus is on the personnel to pinpoint and delineate the target of interest with the greatest degree of accuracy, aiming to create the best plan for delivering the necessary dose while sparing the healthy tissue. In GATE, the treatment plan should be accurately created and built as several phases of treatment planning are prone to mistakes. The accuracy of dose calculation and delivery must be evaluated for both treatment planning and delivery, and uncertainties in both of these processes can have a significant impact on the overall accuracy of radiotherapy. According to the bar chart in figure 8, the simulation suggested a theoretically attainable outcome since the findings demonstrate a good similarity between the TPS and GATE, with a 1.6% disparity for PTV. The results also revealed

differences of 2.11% for brainstem, 0.16% for spinal cord, and 1.58% for optic chiasm. However, optic nerves recorded higher disparity, which may be due to the organ's closeness to PTV.

A portion of the optic nerve's volume was within the PTV in the TPS configuration, which could lead to an unfavourable dosage level (28). The dosage difference might be caused by inadequate demonstration and simulation of the overlapping structures in GATE. As a result, the dose measured in the GATE setting may be higher than in the TPS setting. The intricacy of the multileaf collimator generated by GATE may also be the cause of this discrepancy in order to match the multileaf collimator predetermined in TPS MONACO. Moreover, multileaf collimator is a geometric component of a linear accelerator that is extremely challenging to simulate in any simulation algorithm. While the MC technique can adequately represent the collimator, doing so is not a simple undertaking. Scaling down is required in the GATE simulation to provide accurate shaping of the multileaf collimator structures because its fixed geometry was specified during planning, possibly explaining the existence of variances.

When necessary, PRV provides a margin around OAR to take setup, motion, and anatomy differences into account (38). By purposefully limiting an area to a lower dose, PRV will better shape dose distributions and further assure the sparing of healthy OARs. All OARs and PTV were within the dose constraints, with the exception of the parotid glands. Creating a structure that allows critical OAR to be deducted from the target region when it is prescribed with a higher dosage than the tolerance of the overlapping OAR is one approach to prevent the OAR from receiving doses that are higher than the dose limit. To maximise the therapeutic ratio of treatment, this strategy may, however, lead to a compromise between proper tissue sparing and effective treatment of the target (39). In this work, whole brain radiotherapy was performed, which is considered a palliative treatment. Due to lower radiation doses and shorter patient life expectancies, exposures to OARs are sometimes deemed less significant in palliative settings. These needless radiation exposures eventually jeopardise the patient rather than treating the cancer. However, in a palliative situation, reirradiation and higher-dose stereotactic therapies are the common approaches in metastatic cases. During this scenario, unintentional toxicity could happen if cumulative normal tissue dosage restrictions are not adhered (39). In this work, it is evident that the utilisation of GATE with sophisticated computer algorithms can be a useful tool for the verification of treatment planning, and with the advancement of technology and algorithms, it is vital to step back and adopt a novel approach to improve treatment (40).

CONCLUSION

The results revealed the potential of MC GATE simulation in the dosimetric evaluation and verification of the treatment planning in brain radiotherapy using a custom-made head phantom. For the majority of the volume of interest, the doses predicted by TPS and MC simulation were in close proximity. These outcomes can be attributed to the calculating algorithms' shortcomings in both TPS and MC.

ACKNOWLEDGEMENT

The authors acknowledged Universiti Kebangsaan Malaysia and Universiti Sains Malaysia for allowing this study to be conducted.

Funding: Geran Galakan Penyelidik Muda (GGPM-2023-027), Universiti Kebangsaan Malaysia, Universiti Sains Malaysia Short-Term Grant (304/PFIZIK/6315322) and Universiti Sains Malaysia Bridging Grant (304.PPSK.6316324).

Ethical consideration: N/A

Author contribution: Conceptualisation: N.H., Z., F.Y.; Data curation: H., F.R., H., S.; Formal analysis: H., F.R.; Funding acquisition: N.H., F.Y.; Investigation: F.R., H., S., H., S.; Methodology: H., F. R., H.; Project administration: N.H., Z., F.Y.; Resources: N.H., F.Y., Z.; Software: F.R., N.H.; Supervision: N.H., Z., F.Y.; Validation: N.H., F.R., A.; Visualisation: S.H., F.R.; Original draft: S.H.; Writing – review & editing: S.H., F.R., A.

REFERENCES

1. Bilimaga RS, Nirmala S, Rishi KS, Janaki M, Ponni A, Rajeev A, et al. (2009) Role of palliative radiotherapy in brain metastases. *Indian J Palliat Care*, **15**(1): 71-5.
2. Antonadou D (2005) Current treatment of brain metastases. *Bus Brief Eur Oncol Rev*.
3. Souza VGP, de Araújo RP, Santesso MR, Seneda AL, Minutentag IW, Felix TF, et al. (2023) Advances in the molecular landscape of lung cancer brain metastasis. *Cancers*, **15**(3): 722.
4. Tsao MN, Lloyd N, Wong R, Chow E, Rakovitch E, Laperriere N (2006) Whole brain radiotherapy for the treatment of multiple brain metastases. *Cochrane database Syst Rev*, **3**: CD003869.
5. Siker ML and Mehta MP (2007) Radiation for brain metastases. *Cancer Treat Res*, **136**: 91-115.
6. Nevelsky A, Ieumwananonthachai N, Kaidar-Person O, Bar-Deroma R, Nasrallah H, Ben-Yosef R, et al. (2013) Hippocampal-sparing whole-brain radiotherapy using Elekta equipment. *J Appl Clin Med Phys*, **14**(3): 4205.
7. Fielding AL (2023) Monte-Carlo techniques for radiotherapy applications I: introduction and overview of the different Monte-Carlo codes. *J Radiother Pract*, **22**: e80.
8. Jan S, Santin G, Strul D, Staelsens S, Assié K, Autret D, et al. (2004) GATE: a simulation toolkit for PET and SPECT. *Phys Med Biol*, **49** (19): 4543-61.
9. Jan S, Benoit D, Becheva E, Carlier T, Cassol F, Descourt P, et al. (2011) GATE V6: a major enhancement of the GATE simulation platform enabling modelling of CT and radiotherapy. *Phys Med Biol*, **56**(4): 881-901.
10. Agostinelli S, Allison J, Amako K al, Apostolakis J, Araujo H, Arce P, et al. (2003) GEANT4—a simulation toolkit. *Nucl Instruments methods Phys Res Sect A Accel Spectrometers, Detect Assoc Equip*, **506**(3): 250-303.
11. Tantaoui M, Krim M, Ghazi I, Sobhy Z, Kaanouch O, Moutaoukkil A, et al. (2021) Authentication of a 6 MV varian clinic 2100 using the monte carlo simulation platform GATE/GEANT4. *Hunan Daxue Xuebao/Journal Hunan Univ Nat Sci*, **58**: 9-17.
12. Bosse C, Narayanasamy G, Saenz D, Myers P, Kirby N, Rasmussen K, et al. (2020) Dose calculation comparisons between three modern treatment planning systems. *J Med Phys*, **45**(3): 143-7.
13. Radaideh KM (2017) A custom made phantom for dosimetric audit and quality assurance of three-dimensional conformal radiotherapy. *J Sains Nukl Malaysia*, **24**(1): 48-58.
14. Zuber SH, Hashikin N, Mohd Yusof MF, Hashim R (2020) Lignin and Soy Flour as Adhesive Materials in the Fabrication of Rhizophora spp. Particleboard for Medical Physics Applications. *J Adhes*, **98**(5): 429-448.
15. Zuber S, Hashikin N, Yusof MFM, Aziz MZA, Hashim R (2021) Influence of different percentages of binders on the physico-mechanical properties of Rhizophora spp. particleboard as natural-based tissue-equivalent phantom for radiation dosimetry applications. *Polymers (Basel)*, **13**(11): 1868.
16. Zuber SH, Yusof MFM, Hashikin NAA, Samson DO, Aziz MZA, Hashim R (2021) Rhizophora spp. as potential phantom material in medical physics applications – A review. *Radiat Phys Chem*, **189**: 109731.
17. Zuber SH, Hashikin NAA, Mohd Yusof MF, Hashim R (2020) Physical and mechanical properties of soy-lignin bonded Rhizophora spp. particleboard as a tissue-equivalent phantom material. *Bio-Resources*, **15**(3): 5558.
18. Zuber SH, Hashikin NAA, Mohd Yusof MF, Aziz MZA, Hashim R (2021) Characterization of soy-lignin bonded Rhizophora spp. particleboard as substitute phantom material for radiation dosimetric studies - Investigation of CT number, mass attenuation coefficient and effective atomic number. *Appl Radiat Isot Incl data, Instrum methods use Agric Ind Med*, **170**: 109601.
19. Papanikolaou N, Battista J, Boyer A, Kappas C, Klein E, Mackie T, et al. (2004) Tissue inhomogeneity corrections for megavoltage photon beams. *AAPM Report No. 85, Task Group No 65 of the Radiation Therapy Committee of the American Association of Physicists in Medicine*.
20. Brennan SM, Thirion P, Buckney S, Shea CO, Armstrong J (2010) Factors influencing conformity index in radiotherapy for non-small cell lung cancer. *Med Dosim Off J Am Assoc Med Dosim*, **35** (1): 38-42.
21. Prescribing I (1993) Recording and reporting photon beam therapy. *ICRU Report 50. Bethesda, MD Int Comm Radiat Units Meas*.
22. Shaw E, Kline R, Gillin M, Souhami L, Hirschfeld A, Dinapoli R, et al. (1993) Radiation Therapy Oncology Group: radiosurgery quality assurance guidelines. *Int J Radiat Oncol Biol Phys*, **27**(5): 1231-9.
23. Schneider W, Bortfeld T, Schlegel W (2000) Correlation between CT numbers and tissue parameters needed for Monte Carlo simulations of clinical dose distributions. *Phys Med Biol*, **45**(2): 459.
24. Chetty IJ, Rosu M, Kessler ML, Fraass BA, Ten Haken RK, Kong F-MS, et al. (2006) Reporting and analyzing statistical uncertainties in Monte Carlo-based treatment planning. *Int J Radiat Oncol Biol Phys*, **65**(4): 1249-59.
25. Zuber SH, Hashikin NAA, Mohd Yusof MF, Hashim R (2020) Investigation on Suitable Coating Material for Soy-lignin bonded Rhizophora spp. Particleboard for Medical Physics Applications. *Bioresour*, **15**(4): 7404.
26. Reynaert N, van der Mark S, Schaart D (2006) Monte Carlo Treatment Planning—An Introduction. *Nederlandse Commissie Voor Stralingsdosimetrie*.
27. Sechopoulos I, Rogers DWO, Bazalova-Carter M, Bolch WE, Heath EC, McNitt-Gray MF, et al. (2018) RECORDS: improved Reporting of monte Carlo RaDiation transport Studies: Report of the AAPM Research Committee Task Group 268. *Med Phys*, **45**(1): e1-5.
28. Schlaechter M, Raidou R, Muren LP, Preim B, Putora PM, Bühl K (2019) State-of-the-Art Report: Visual Computing in Radiation Therapy Planning. *Comput Graph Forum*, **38**: 753-79.
29. Feuvret L, Noël G, Mazeron J-J, Bey P (2006) Conformity index: a review. *Int J Radiat Oncol Biol Phys*, **64**(2): 333-42.
30. Salimi M, Abi KST, Nedaie HA, Hassani H, Gharaati H, Samei M, et al. (2017) Assessment and comparison of homogeneity and conformity indexes in step-and-shoot and compensator-based intensity modulated radiation therapy (IMRT) and three-dimensional conformal radiation therapy (3D CRT) in prostate cancer. *J Med Signals Sens*, **7**(2): 102-7.
31. Jabbari K, Azarmahd N, Babazade S, Amouheidari A (2013) Optimizing of the tangential technique and supraclavicular fields in 3

dimensional conformal radiation therapy for breast cancer. *J Med Signals Sens*, **3**(2): 107–16.

- 32. Arora RD and Casella M (2021) Palliative radiation therapy for brain metastases. In *Treasure Island (FL)*. StatPearls Publishing; 2023 Jun 4.
- 33. Monti AF, Ostinelli A, Frigerio M, Cosentino D, Bossi A, Cazzaniga LF, et al. (1995) An ICRU 50 radiotherapy treatment chart. *Radiat Oncol*, **35**(2): 145-50.
- 34. Papanikolaou N, Battista J, Boyer A, Kappas C, Klein E, Mackie T, et al. (2004) Tissue inhomogeneity corrections for megavoltage photon beams. *AAPM Report No 85; Task Group No. 85; Task Group No. 65*.
- 35. Chin DWH, Treister N, Friedland B, Cormack RA, Tishler RB, Makrigiorgos GM, et al. (2009) Effect of dental restorations and prostheses on radiotherapy dose distribution: a Monte Carlo study. *J Appl Clin Med Phys*, **10**(1): 80-9.
- 36. Spirydovich S, Papiez L, Langer M, Sandison G, Thai V (2006) High density dental materials and radiotherapy planning: comparison of the dose predictions using superposition algorithm and fluence map Monte Carlo method with radiochromic film measurements. *Radiat Oncol*, **81**(3): 309-14.
- 37. Gagne I, Zavgordni S (2007) Evaluation of the analytical anisotropic algorithm (AAA) in an extreme water-lung interface phantom using Monte Carlo dose calculations. *J Appl Clin Med Phys*, **8**(1): 33-46.
- 38. Hodapp N (2012) The ICRU Report 83: prescribing, recording and reporting photon-beam intensity-modulated radiation therapy (IMRT). *Strahlenther Onkol*, **188**(1): 97-9.
- 39. Wright JL, Yom SS, Awan MJ, Dawes S, Fischer-Valuck B, Kudner R, et al. (2019) Standardizing normal tissue contouring for radiation therapy treatment planning: An ASTRO consensus paper. *Pract Radiat Oncol*, **9**(2): 65-72.
- 40. Malicki J (2012) The importance of accurate treatment planning, delivery, and dose verification. *Reports Pract Oncol Radiother J Gt Cancer Cent Pozn Polish Soc Radiat Oncol*, **17**(2): 63-5.